

Magma flow in the East Greenland dyke swarm inferred from study of anisotropy of magnetic susceptibility: magmatic growth of a volcanic margin

Jean-Paul Callot^{1,2,*} and Laurent Geoffroy²

¹Laboratoire de Géologie, CNRS UMR 8538, Ecole Normale Supérieure, 24 rue Lhomond, 75231, Paris cedex 5, France

²Laboratoire de Géodynamique des Rifts et des Marges Passives, EA 3064, Université du Maine, 72017 Le Mans cedex, France

Accepted 2004 July 21. Received 2004 July 2; in original form 2004 April 1

SUMMARY

Volcanic passive margins (VPMs) are characterized by large volumes of melt emplaced within the lithosphere during break-up processes. Several data and a recently proposed conceptual model of volcanic margin development suggest that VPMs are fed from localized crustal zones of magma storage, underlying large polygenetic volcanoes localized above diapir-like instabilities of the asthenosphere. We investigated the magma flow pattern within the coast-parallel dyke swarm of the East Greenland VPM, which is the only outcropping VPM, over a distance of 125 km. The 44 sampled dykes are representative of the successive families of intrusions. Igneous petrofabrics are constrained by the measurements of the anisotropy of magnetic susceptibility. The magnetic fabrics are of medium to low anisotropy ($P' < 1.08$) and show moderately oblate ellipsoids ($T > 0$). Flow-related fabrics are recorded in 75 per cent of the sampled dykes. We infer the flow directions from the imbrication geometry of the magnetic foliation planes at the dyke margins, and check the results by measuring the preferred orientation of plagioclase in thin sections cut in the magnetic principal planes. Due to probable fabric superposition, the magnetic lineation represents the zone axis for the distribution of magnetic foliation plane. We obtained 23 reliable flow directions that are predominantly horizontal and directed away from identified crustal reservoirs. This flow pattern supports the proposed model of VPM growth, and emphasizes the localized nature of the magma sources in the mantle. The entire flood basalt sequence appears to have been fed by a restricted number of crustal reservoirs and associated dyke swarms.

Key words: anisotropy of magnetic susceptibility, dyke, flood basalt, Greenland, large igneous province, North Atlantic, plume, volcanic margin.

1 INTRODUCTION

The ratio of the induced magnetization of a material to the external applied field defines the bulk magnetic susceptibility. Due to crystallographic properties and spatial distribution of minerals and mineral shapes, the magnetic susceptibility is anisotropic and gives an estimate of the petrofabric, averaged over all sources in the entire rock sample (e.g. Tarling & Hrouda 1993). The high sensitivity of anisotropy of magnetic susceptibility measurements (AMS; anisotropy of 0.1 per cent down to a susceptibility of 10^{-7} SI) allows the determination of magnetic fabrics in apparently isotropic rocks. AMS has thus been used to quantify rock fabric and in some case to provide an estimation of finite strain, in several geological settings:

sedimentary, metamorphic and igneous (e.g. Rochette *et al.* 1992, 1999; Borradaile & Henry 1997).

Practically all magmatic rocks show a petrofabric, or texture, even if it is not easily distinguished in the field (e.g. Bouchez 1997). Several mechanisms accounting for the emplacement dynamics and subsequent cooling and solid state evolution are responsible for the fabric development (Nicolas 1992). The mineral fabric of a magmatic rock can be related to (1) gravitational sedimentation of crystals, (2) shearing of a viscous magma containing rigid particles during emplacement and (3) post-cooling plastic deformation. Rocks deformed in the magmatic state, which are characterized by a preferred orientation of grain shape, are easily distinguished from plastically strained rocks, characterized by preferred orientations of crystal lattices. Nevertheless, rocks strained in the magmatic state also present strain-induced structures similar to those observed in plastically strained metamorphic and sedimentary rocks, such as SC fabrics (e.g. Nicolas 1992; Callot & Guichet 2003).

*Now at: Institut Français du Pétrole, 1-4 av. de Bois Préau, 92852 Rueil-Malmaison cedex, France. E-mail: j-paul.callot@ifp.fr

Since the early studies made by Graham (1954) and Khan (1962), AMS has been widely used to reveal the internal magmatic structure of plutonic rocks, principally para- and ferromagnetic granites (e.g. Bouchez 1997). The easy and quick use of AMS has ensured its increasing success, and numerous plutons have been structurally mapped, showing the high spatial homogeneity of their texture and the ability of AMS to retrieve a rock fabric from a small number of samples. These results have also been successfully compared with numerical and experimental modelling of texture acquisition (Ježek *et al.* 1996; Arbaret *et al.* 1997). Similarly, AMS has been used in mafic rocks (dykes, sills lava flows), particularly basaltic dykes, but its use here is more controversial (Ellwood 1978; Canon-Tapia *et al.* 1997; Dragoni *et al.* 1997; Callot 2002).

In the present paper we aim to study the flow dynamics within a volcanic margin dyke swarm to constrain the magma transfer in the upper crust during continental break-up associated with (or triggered by) a mantle plume (e.g. White & McKenzie 1989; Richards *et al.* 1989). We shall first present in detail the main characteristics of the East Greenland volcanic margin and its relationship with the Icelandic Plume. The methodology, based on the measurement of the AMS, relies on the orientation of the magnetic foliation plane (Hillhouse & Wells 1991; Geoffroy *et al.* 2002). This methodology has rarely been applied to dykes and will be discussed (Moreira *et al.* 1999; Aubourg *et al.* 2002). We will finally discuss the possible implications of our results on the general issue of the interaction between an active upwelling of mantle material and the break-up processes of continental lithosphere.

2 THE NORTH ATLANTIC VOLCANIC PROVINCE AND THE EAST GREENLAND MARGIN

2.1 Mantle plumes, large igneous provinces and volcanic passive margins

Volcanic passive margins (VPMs) belong to the so-called large igneous provinces (LIPs). When associated with a hotspot track, and with an abnormally thick oceanic crust, a volcanic margin records the break-up of continental lithosphere over a mantle plume (e.g. White & McKenzie 1989; Hill 1991; Coffin & Eldholm 1994; Anderson 1994; Eldholm *et al.* 1995; Courtillot *et al.* 1999).

Since the seminal paper by Morgan (1972), several models of interaction between mantle plumes and lithosphere have been discussed. White & McKenzie (1989) suggest a passive mode of rifting, the mantle plume ascent and melting being controlled by the thinning of the lithosphere below the rift zones. The mantle plume plays a much more active role in the model of Richards *et al.* (1989), by thinning the lithosphere through thermal and convective erosion. Here the development of plateau basalt precedes the rifting event. By suggesting that lateral thermal and compositional contrasts in the continental lithosphere could drive small-scale convective cells and enhance local mantle melting, Anderson (1994) questioned systematically the role of the plume. Eventually, the comprehensive review of Courtillot *et al.* (1999) put forward a causal link between mantle plume activity, onshore trap emplacement and subsequent rifting of the lithosphere, associated with the development, along the rift zone, of a VPM, as a driving mechanism for plate break-up and plate tectonics.

VPMs exhibit strong differences from classic non-volcanic margins, particularly the large volumes of both extrusive and intrusive igneous products accompanying lithospheric break-up (Eldholm &

Grue 1994). These products include: (1) thick lava flow sequences forming flat-lying or seaward-dipping basaltic flows onshore and seaward-dipping basalts and tuffs offshore (Hinz 1981); (2) central intrusive complexes; (3) coast-parallel dyke swarms centred on complexes (Myers 1980); (4) variable volumes of underplated material with high seismic velocity (e.g. Korenaga *et al.* 2000).

2.2 The Thulean province: evidence for localized melting zones

The impact of the Icelandic mantle plume has long been considered as the origin for the Thulean magmatic province (Fig. 1) Holmes (1918) which was emplaced in the early Palaeocene. The onshore basalt represents roughly $0.4 \times 10^6 \text{ km}^3$ (principally, on the Blossesville Promontory, the West Coast of Greenland and the British and Faeroe Isles). Offshore, the seaward-dipping reflectors represent more than $1.8 \times 10^6 \text{ km}^3$, and the underplated mafic body and igneous crust (if assumed to be entirely magmatic in nature) roughly $4.8 \times 10^6 \text{ km}^3$, ranking the Thulean province as among the largest LIPs (Eldholm & Grue 1994).

The East Greenland margin has been widely studied, both offshore (ODP leg 152) and onshore, and a large collection of dating is available, especially from inland exposure where the syn-magmatic flexing of the lava flows toward the sea is well expressed (Wager & Deer 1938; Nielsen 1978). Fig. 2 summarizes the magmatic chronology. The first magmatic episode is dated at 62 Ma, as is the case over the entire Thulean province. This short event ($\sim 2 \text{ Myr}$) corresponds to the main plateau basalt and picrites on the west coast of Greenland, the lower series of the Blossesville Promontory, the lower series offshore in the North Atlantic and the first lava in Scotland, associated with the earliest activity of some of the central intrusive complexes (Tegner *et al.* 1998; Torsvik *et al.* 2001). In East Greenland this episode is followed at 55 Ma by the main event, associated with continental break-up, and a strong focusing of the lava emission along the future ridge axis. The main lava onshore and the main part of the seaward-dipping reflectors offshore are deposited with major magmatic activity at several plutonic complexes associated with the main dyke swarm. A third episode of magmatic activity is marked by the emplacement of post-flexure dykes, and of several plutonic intrusions along the East Greenland margin at $\sim 50 \text{ Ma}$. These data show the temporal persistence of magmatic activity at several locations throughout the three main effusive episodes, separated by a zone lacking magmatic activity (Fig. 2). This illustrates the persistence of localized melting—or magma transfer—zones within the lithosphere.

The early lavas of the Thulean province are characterized by a high MgO content (8–20 per cent) on both side of Greenland, in the North Atlantic and in Scotland (Scarraw & Cox 1995; Fitton *et al.* 1998). Such picrites suggest a high potential temperature of the melting mantle ($\sim 1450 \text{ }^\circ\text{C}$), typical of a mantle plume environment. The primary melts (early lava from the first pulse) have been formed at great depth (80–110 km for the Hebrides and Greenland lava) with a low degree of melting (alkaline lava). These are followed by the main tholeiitic lavas (corresponding to the second episode), formed at a shallower depth ($\sim 50 \text{ km}$) at a higher degree of melting ($\sim 20 \text{ per cent}$) from a depleted mantle (Kerr 1994), and differentiated in crustal storage zones ($\sim 8 \text{ kbar}$, Fram & Leshner 1997). This dramatic decrease in melting depth (almost 50 per cent) within a very short period of time ($\sim 5 \text{ Myr}$) shortly before or during the main tectonic episode has been described in several LIPs (e.g. White & McKenzie 1995).

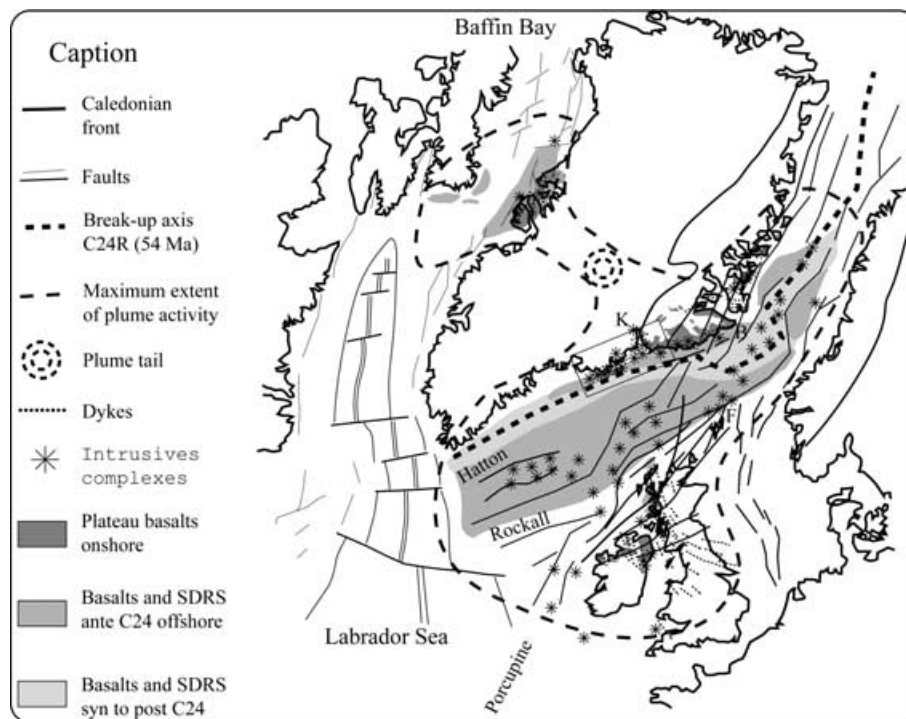


Figure 1. Regional setting of the North Atlantic volcanic province at magnetic chron 24 (~55 Ma) (after Callot 2002). B, Blossville promontory; K, Kangerlussuaq Fjord; F, Faeroe Islands. Note the distribution of the magmatic product at the time of break-up. The location of the mantle plume tail and deep distribution of melt is after Nielsen *et al.* (2002) and Callot (2002).

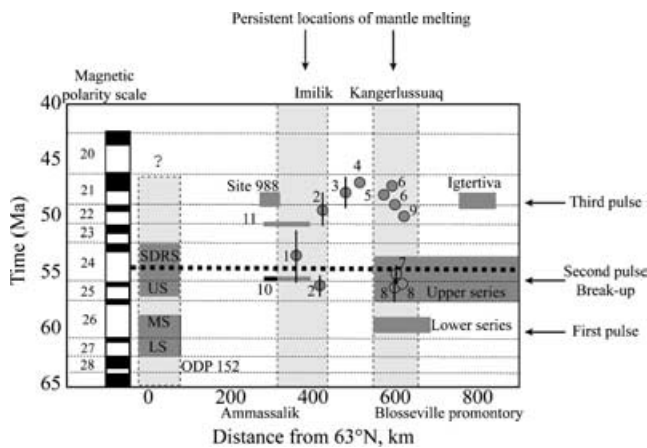


Figure 2. Summary of magmatic events along the east coast of Greenland, after Tegner *et al.* (1998); data from Sinton & Duncan (1998), Tegner *et al.* (1998) and Lenoir *et al.* (2002). 1, Kap Gustav; 2, Imilik; 3, Kruuse Fjord; 4, Igtutarajik; 5, Nordre Aputitek; 6, Kap Edward; 7, Skaergaard; 8, Sorgenfrigletscher Sill complex; 9, Liloise Bjerge; 10, pre-flexure dyke swarm; 11, post-flexure dyke swarm. Note the existence of a localized zone of persistent activity (see text for details). L, M, US: lower, middle and upper series of lava from the ODP leg 152.

2.3 Proposed model and aim of the study

This quick thinning of the lithosphere, apparently associated with the development of long-lived intrusive complexes, is a major characteristic of LIPs and VPMs. A plate tectonic process cannot reasonably explain such thinning, which is therefore likely to be of local origin and may express the thermomechanical interaction between the plume material and the base of the lithosphere (Fleitout *et al.* 1986;

Geoffroy 1998, 2001). On the basis of previous considerations and extensive field work, Geoffroy (1998, 2001) suggest that a small-scale, thermally driven convection in the plume head could lead to quick erosion of the lithosphere at localized spots which define the persistent mantle melting zone (see also Callot *et al.* 2001a). The magma reservoirs associated with these melting zones in turn localize both magmatic accretion, through lateral injection of dykes, and distension within the crust.

The mechanical effect of such low-resistance bodies built in the lithosphere has already been tested and can account for the bulk initiation and propagation of a rift segment (Callot *et al.* 2001a, 2003). In the present study we will focus on the magmatic growth of a VPM. The model of Geoffroy (2001) assumes lateral injection of evolved magmas from the crustal reservoirs within the dyke swarms. This may be tested using AMS data to estimate the directions of magma flow within the coast-parallel dyke swarm of the East Greenland margin, which offers the only opportunity for such a study.

2.4 The onshore East Greenland margin

The structure of East Greenland margin is well exposed, including levels close to the palaeotopographic surface down to the internal part of the dyke swarms and magma centres (Figs 2 and 3) Myers (1980); Klausen (1999). This is due to Tertiary differential uplift/erosion (Clift *et al.* 1998) and more recent glacial erosion. The continental part of the volcanic margin crops out from Kangerlussuaq to Ammassalik, 100 km west of the continent-ocean transition (Fig. 3b) Korenaga *et al.* (2000).

South of Kangerlussuaq Fjord (Fig. 3), the lava pile and possibly underlying Mesozoic sediments have been removed by erosion so that the mafic dyke swarms that fed the lava crop out parallel to the coast. The southern part of the margin exhibits two major

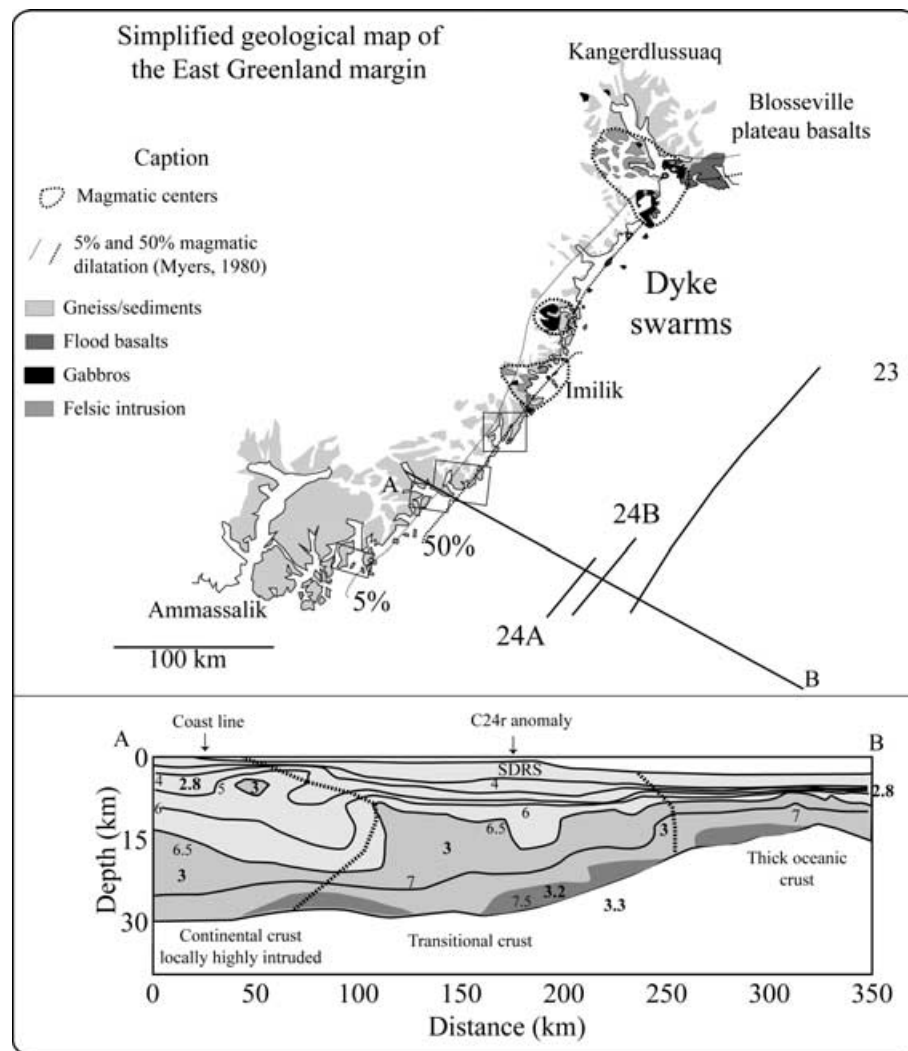


Figure 3. Top: simplified geological map of the southern part of the East Greenland volcanic margin with location of the studied zones. Bottom: interpretative seismic cross-section of the margin after Korenaga *et al.* (2000). Bold numbers for rock densities, light numbers for P -wave velocities. Shading and lines interpolates seismic velocities.

hypovolcanic complexes known as the Kruuse Fjord and the Imilik–Qialineq gabbros and syenites. There is no evidence to support the existence of any other major complex south of Imilik–Qialineq. The coastal dyke swarm of East Greenland is roughly 400 km long, and is composed of outcrop of ~ 400 dykes across the strike. The dykes generally trend north–south to N040, with the swarm showing a symmetrical *en echelon* arrangement apart from the two igneous centres (Figs 3b and 4) Myers (1980), which is also apparent on aeromagnetic surveys offshore to the south (Larsen 1978). The crustal flexure is marked by a seaward increase in the tilt of the earliest dykes, which are assumed to have been injected vertically (Myers 1980; Karson & Brooks 1999).

The dykes' continentward dips, which express the crustal flexure of the margin, vary both along the strike and across the strike of the swarm. Firstly the mean dip of the dykes increases along-strike, from the less flexed part of the margin south of Kap Wandel, where the dykes are subvertical, to the northern zone around the Kap Gustav intrusive complex, where the mean dip reaches more than 25° (Fig. 4a). Secondly, we observe along each transect across the swarm a remarkable increase in both (1) the cumulative magmatic dilatation, from less than 1 per cent in the inland part of the

swarm where dykes are vertical (Erik Den Rodes and Sarternit Island) to more than 50 per cent along the coastline (at Kap Wandel for example), and (2) the seaward tilt of the early dykes. The dykes display variable dips indicating syn-flexure emplacement (Karson & Brooks 1999; Klausen 1999). The study of the thickness variation along-strike had led Klausen & Larsen (2002) to propose a lateral propagation of the dykes from between the crustal igneous centres, implying a lateral feeding of the swarm.

At Kap Wandel three contrasted generations of intrusions crop out, exhibiting constant petrological characteristics (Fig. 5a). The earlier magmas of alkaline affinity, associated with picrite basalt, are not well exposed, and the associated feeder dykes are poorly documented (Klausen 1999). Most of the dykes belong to the earliest (pre-flexure) generation, and show a tholeiitic affinity (Table 1) which correlates well with the main THOL1 and THOL2 coast-parallel dyke swarms described further north by Nielsen (1978). These doleritic dykes are relatively thin (up to 9 m thick, 4.5 m on average), with up to 40 per cent of andesine–labradorite plagioclase (Fig. 5b). The dykes of this first generation generally trend N030, and are tilted oceanwards by the seaward coastal flexure. They are cross-cut by a second generation of thicker (from 15 to 30 m)

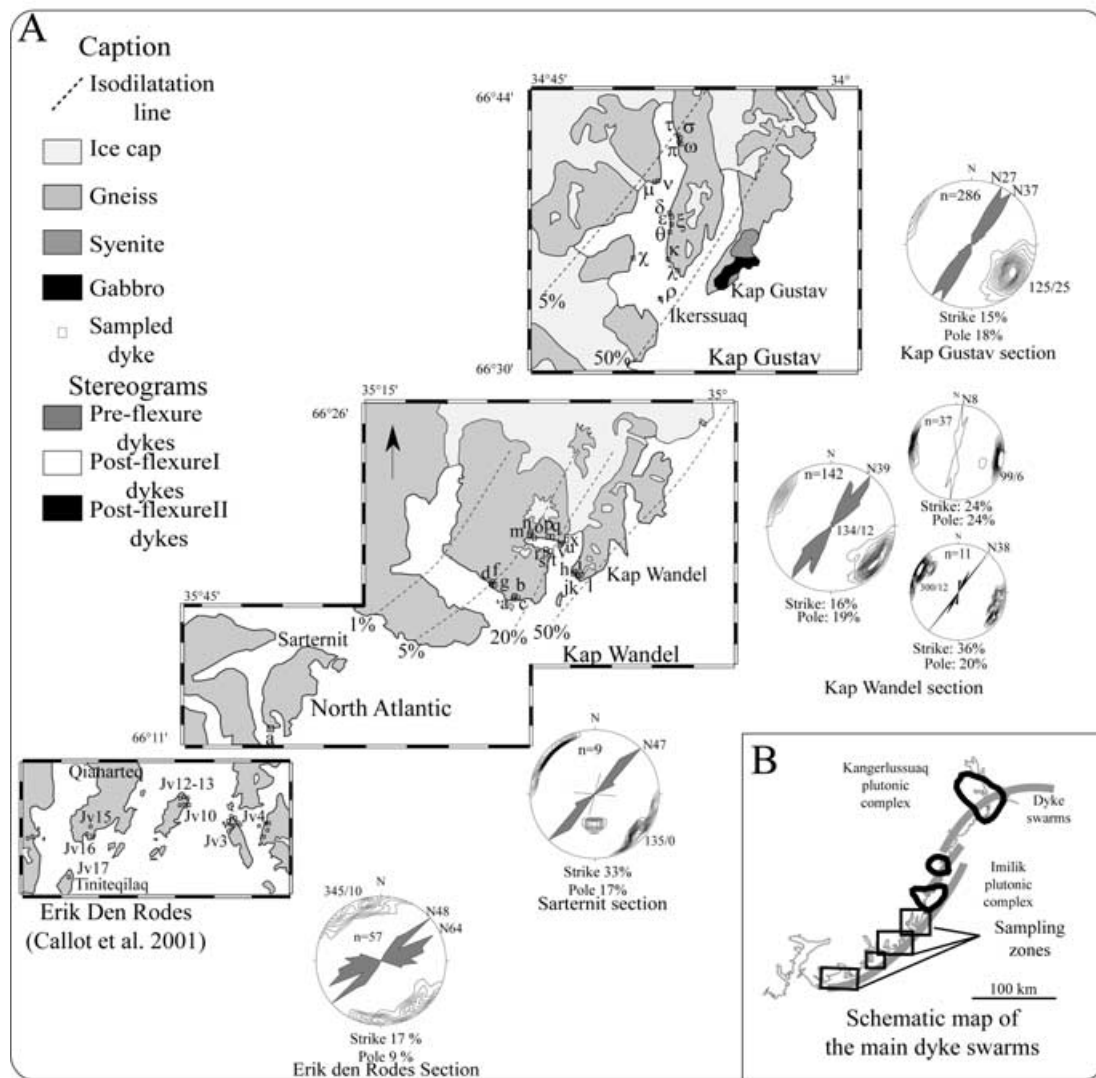


Figure 4. (a) Detailed maps of the studied zones with the location of the sampled dykes. The stereograms (Stereonet©, lower hemisphere projection) show the orientation roses together with the mean poles for the dykes (with the contoured density distribution incremented every 1 per cent). The three intrusion generations are indicated for the Kap Wandel area; n is the number of measured dykes, and the mean strike and pole are given on the plot. (b) Schematic view of the main dyke swarms and plutonic complexes.

alkaline dykes trending N010 which post-date the flexure (post-flexure type I, Table 1, Figs 4 and 5c). These dykes exhibit a porphyritic texture with plagioclase phenocryst 400–1500 μm in length. A late generation of scarce and thin differentiated dykes of alkaline affinity is seen to cross-cut the two earlier generations (post-flexure II type, Fig. 5d).

3 THE USE OF ANISOTROPY OF MAGNETIC SUSCEPTIBILITY IN DYKES

3.1 General considerations

Under low-field conditions the anisotropy of magnetic susceptibility (AMS) can be linearly approximated by a second-order tensor, whose three eigenvectors ($K_1 > K_2 > K_3$) define the magnetic ellipsoid. AMS measures all contributions due to dia-, para- and ferromagnetic (*sensu lato*) minerals, averaged over a rock sample. The main sources of anisotropy are the anisotropic shape of miner-

als, their crystallographic anisotropy and the anisotropic distribution of shape orientation in the rock sample (Stacey 1960; Bhattacharya 1971; Hargraves *et al.* 1991; Rochette *et al.* 1992). In AMS measurement the signal is averaged over a rock sample of $\sim 10 \text{ cm}^3$; thus it not only estimates the grain-scale AMS averaged over the total number of grains (shape and crystallographic AMS), but it also integrates the anisotropic relative distribution of shape (which we may call the sample effect) (Stephenson *et al.* 1986). In so doing AMS is a true estimate of the petrofabric, i.e. the texture, although it is generally interpreted in term of grain effects only.

Following the observations and modelling of Blanchard *et al.* (1979), Knight & Walker (1988) first documented, with AMS data, the imbrication fabric of elongated ferromagnetic particles along the chilled margins of basaltic dykes, which allows one to draw the flow direction. The paramagnetic minerals mainly define the texture, whereas the ferromagnetic oxides dominate the AMS signal due to their high susceptibility. Although they are often late-stage (i.e. post-flow) crystallization products in basaltic magmas, their anisotropic distribution within the silicate template should also reflect the

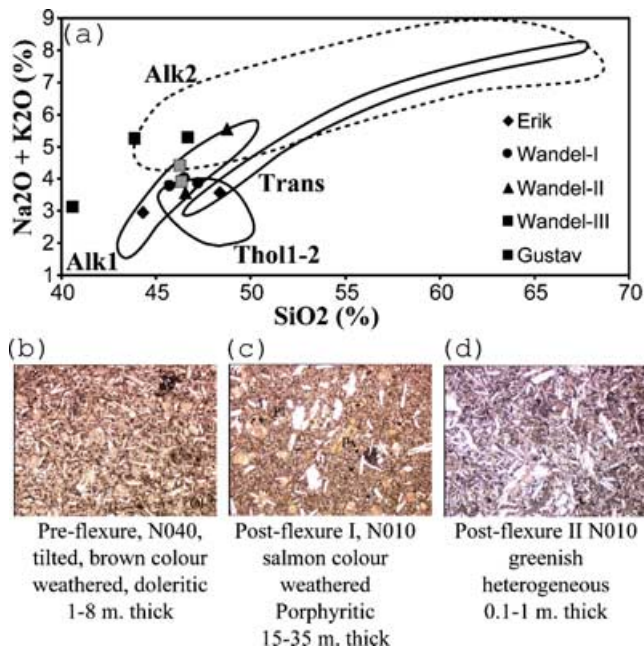


Figure 5. (a) Alkalis versus silica diagram for the analysed dykes (Table 1) together with the results of Nielsen (1978). Thin sections show the contrasted petrographic textures of the three dyke generations. (b) Doleritic texture of pre-flexure tholeiitic dykes. (c) Porphyritic texture of thick alkaline dykes belonging to post-flexure I family. (d) Heterogeneous texture with phenocrysts of plagioclase and pyroxene, typical of the post-flexure II alkaline dykes.

flow-related magmatic texture (Hargraves *et al.* 1991). Unless the fabric is controlled by single-domain particles, one expects the maximum susceptibility axes to define the flow direction. Several studies have shown concordance between the magnetic axis K_1 (due to the ferromagnetic oxides) and external flow indicators such as phenocrysts or elongated xenoliths (Staudigel *et al.* 1992; Varga *et al.* 1998).

Nevertheless, field studies and numerical experiments have emphasised possible discrepancies between the magnetic lineation and the assumed flow-related texture (Ellwood 1978; Baer 1995; Moreira *et al.* 1999; Geoffroy *et al.* 2002; Callot & Guichet 2003). It is interesting to note that following Rochette *et al.* (1992), the vast majority of authors consider as indicative of a flow-related magnetic fabric the 'normal magnetic fabrics', i.e. dykes with a magnetic foliation plane close to the dyke plane, which generally have a rather

oblate magnetic texture (for a compilation of published data see Callot & Guichet 2003, and Fig. 11). In such dykes, the pole of magnetic foliation K_3 is usually better defined than the magnetic lineation K_1 , which, however, is used to infer the flow direction. These fabrics, which are generally of low anisotropy, are prone to fabric superposition and composition (Housen & Van der Pluijm 1993; Henry 1997; Callot & Guichet 2003). In particular, Geoffroy *et al.* (2002) have shown that for more than 60 per cent of the studied samples from a case study in Greenland the magnetic lineation, i.e. the inferred flow direction, is perpendicular to the mean elongation of plagioclase phenocryst, i.e. the assumed real flow direction. This can easily be modelled as the result of the superposition at the plug scale, of SC-type fabric, the macroscopic K_1 being the zone axis of the SC fabrics (Henry 1997; Callot & Guichet 2003).

3.2 The foliation methodology for estimating the flow vector and confidence ellipse

We will focus here on normal fabric dykes (*sensu* Rochette *et al.* 1991). As proposed by Geoffroy *et al.* (2002), the flow direction is inferred geometrically from the imbrication, at the dyke margin, of the magnetic foliation plane (Fig. 6a). This is close to the methodology used by numerous authors (e.g. Knight & Walker 1988), but it avoids the possible misuse of K_1 as a flow lineation. Some other authors have inferred flow direction in a comparable manner for tuffs and lava flows (Hillhouse & Wells 1991; Canon-Tapia *et al.* 1997; Palmer & MacDonald 1999).

The flow direction is calculated at two scales (see Geoffroy *et al.* 2002). First, a local flow vector is obtained for each pair of measured plugs and the oriented margin close to the plug. A mean for the pool of local flow vectors is calculated for each dyke margin, using a classical Fisher statistic (the so-called 'local flow vector'). Second, for each dyke margin, a mean flow vector for the margin is calculated from the mean magnetic foliation plane (Jelinek 1978) and the average margin orientation ('mean flow vector'). In that case, the confidence interval is estimated by a random generation of pairs of poles of foliation and dyke margins, within their own confidence interval (the 95 per cent-ellipse for K_3 , and an arbitrary estimate of the orientation error for the margin, usually 5–10°). This distribution of 'possible flow vectors' delineates the confidence interval (Fig. 6b).

Eventually, the data may be compared all together in the dyke reference frame (Rochette *et al.* 1991). In such a case, the dykes are rotated to be vertical and north-south directed, and the data compiled in a single plot. This allows comparison of the data from

Table 1. Chemical analyses of 12 dykes from the different sampling zones and dyke generations (weight per cent of oxides normalized to 100 per cent after correction for water loss).

	Erik		Wandel-I			Wandel-II		Wandel-III			Kap Gustav	
	13G8B	25G5B	M7C	B9C	O6C	U7C	A11B	F10C	C14B	T4B	Θ9C	τ5A
SiO ₂	48.4	44.38	45.8	47.3	46.52	48.8	46.59	44.0	40.8	46.7	46.4	46.36
Al ₂ O ₃	12.0	12.12	12.3	12.9	14.37	11.1	13.48	15.0	11.6	12.9	12.6	13.55
Fe ₂ O ₃	5.7	6.45	4.9	3.9	5.36	5.5	6.28	5.5	8.5	4.2	4.6	5.23
FeO	11.0	14.04	12.5	10.8	11.37	9.8	11.31	9.3	7.2	7.6	11.6	11.95
MnO	0.2	0.31	0.2	0.2	0.26	0.3	0.26	0.2	0.2	0.2	0.2	0.27
MgO	5.8	5.03	5.6	6.4	4.66	8.4	4.92	6.5	8.5	8.6	6.2	4.53
CaO	10.1	9.30	10.0	11.1	9.11	7.0	8.87	11.4	16.1	12.7	10.8	9.30
Na ₂ O	3.0	2.42	3.0	3.2	3.14	4.3	2.86	3.4	1.7	3.3	3.1	3.09
K ₂ O	0.7	0.63	0.8	0.8	0.85	1.3	0.77	1.9	1.52	2.0	0.9	1.36
TiO ₂	2.4	4.70	4.1	2.9	3.67	2.5	4.01	2.2	3.2	1.4	3.1	3.71
P ₂ O ₅	0.6	0.63	0.8	0.6	0.69	1.1	0.65	0.7	0.8	0.4	0.6	0.67
Total	100.0	100.00	100.0	100.0	100.00	100.0	100.00	100.0	100.0	100.0	100.0	100.00

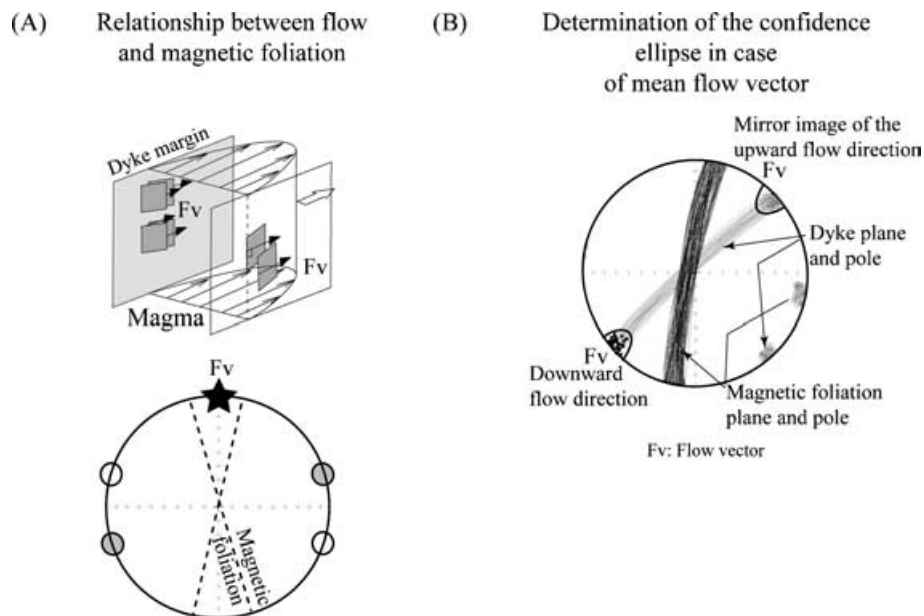


Figure 6. (a) Synthetic diagram illustrating the methodology followed: the flow vector is constructed as the perpendicular to the intersection line between magnetic foliation (assumed to be representative of a planar distribution of phenocrysts) and the dyke margin. (b) Example of the estimation of the confidence ellipse for the margin flow vector. One hundred pairs of mean dyke poles (circles) and mean magnetic foliation poles (diamonds) are drawn and used to construct each a flow vector (open and closed squares). The upward-directed flow vectors have been plotted as downward lineations for the sake of visibility, but all vectors indicate a southwestward-directed flow.

dyke to dyke, and highlights a general pattern of magnetic fabric at the scale of the dyke swarm (see Callot *et al.* 2001a).

Inverse magnetic fabrics, which are geometrically defined as fabrics where the mean magnetic foliation plane is close to being perpendicular to the dyke mean plane, are generally considered as being unrelated to flow. Their origin, either textural, mineralogical or magnetic (monodomain versus single-domain magnetite) remains largely controversial and is under discussion. We here choose to focus on the flow-related fabric and the geodynamic interpretation of the distribution of flow direction.

4 DATA PRESENTATION

4.1 Sampling and methodology

We restricted the study area to the 125 km of the coast-parallel dyke swarm south of the Imilik centre. Following the preliminary study of Callot *et al.* (2001a) (seven dykes sampled), we performed orientation measurements and AMS sampling within the main dyke swarm along two natural transects: Kap Wandel Fjord (23 dykes) and Kap Gustav Fjord (13 dykes, Fig. 4), with some additional data from the Sarternit area (one dyke). We selected dykes (1) with both margins well exposed, (2) unaltered, (3) apparently not inherited from pre-existing fracture sets and (4) less than a few metres thick, when possible, to exclude dykes potentially affected by turbulent or multiple flow (Knight & Walker 1988; Tauxe *et al.* 1998). These dykes belong to each petrographic type and display variable angles of dip. At least seven cores were drilled on both margins of the dykes, as close as possible to the vitrified margins, where we expected the imbrication fabric to be more clearly expressed. In most cases samples and dyke margins at the coring location were oriented using both solar and magnetic compasses. We finally measured the orientation of more than 540 dykes, and drilled 852 cores from 44 dykes along the two transects, which provide ~1170 measurable

plugs (see Table 2). To our knowledge, this constitutes one of the largest AMS datasets involving the petrofabric analysis of a dyke swarm, and the only one dealing with a volcanic margin.

The results were obtained using a KLY3S susceptibility bridge (Geofyzika Brno), which enables a reliable determination of AMS directions down to anisotropy ratios of 1.001. A tensorial statistic, based on linear perturbation analysis (Hext 1963), is applied to determine the mean magnetic axes (Jelinek 1978). Although it may underestimate the errors, the results are similar to those obtained from more complex approaches such as the bootstrap statistical treatment in the case of homogeneous unaltered mafic rocks (e.g. Lienert 1991; Tauxe *et al.* 1998).

4.2 Rock magnetism

We performed susceptibility versus temperature experimental runs ($K-T$ curves) in order to characterize the magnetic mineralogy. The $K-T$ curves are measured with a KLY3-CS3 apparatus (Geofyzika Brno), from 0 to 720 °C, under a controlled atmosphere. The $K-T$ curves obtained under argon and under air are remarkably similar, being almost reversible (Fig. 7a), except for the Erik Den Rødes (Callot *et al.* 2001a) and Sarternit dykes. Oxidation due to atmospheric oxygen results in the presence of haematite. The curves are dominated by Ti-poor titanomagnetite (Curie temperature between 500 and 580 °C). In the case of inverse magnetic fabrics, the dykes display either (1) an irreversible $K-T$ curve (Fig. 7b, dyke 8G), or (2) a curve similar to the one obtained from normal fabric sites (Fig. 7b, dyke Ω) with a higher abundance of maghemite compared with sites displaying normal fabrics. Nevertheless, site 8G may be interpreted as showing a Hopkinson peak associated with a high-Ti magnetite. Inverse magnetic fabrics are thus possibly related either to alteration of the primary magnetic carriers (with production of maghemite) or to particular high-Ti content magnetite. These points deserve a particular treatment which is beyond the scope of the present paper,

Table 2. Magnetic and magnetic susceptibility results for the Kap Wandel and Kap Gustav dykes. $K_{1(3)M(S)}$ indicates the tensorial axis for $K_{1(3)}$ for the northern (southern) margin, K_m indicates Bulk susceptibility. Orientation are given as azimuth (0° – 360°), dip to the right.

Dyke	n/N	K_m	P' (10^{-3} S.D.)	T (10^{-3} S.D.)	K_1 (D/I)	K_3 (D/I)	K_1 (E1)	K_1 (E2)	K_3 (E1)	K_3 (E2)	Trend	Width (m)	K_{1m} (D/I)	K_{3m} (D/I)	K^{1s} (D/I)	K^{3s} (D/I)
A	21/21	34.4	1.023 (1.5)	0.706 (23.7)	191/78	293/2	22	5	12	5	201/78	0.7	0/82	102/2	189/74	303/7
B	23/23	29.3	1.035 (11.4)	0.871 (18.7)	311/81	119/9	31	3	6	3	230/80	5	267/79	125/9	355/72	114/9
C	21/21	83.4	1.002 (6.4)	-0.245 (40.9)	160/15	63/24	53	39	72	48	22/90	0.6	86/32	349/11	165/3	74/28
D	24/24	29.0	1.023 (8.3)	0.857 (16.7)	34/25	125/3	21	5	5	3	32/70	2.2	38/22	128/2	28/32	121/5
F	27/27	61.9	1.021 (8.8)	-0.36 (29.8)	24/54	128/10	8	7	18	7	30/72	0.7	9/55	118/13	40/51	138/9
G	15/18	64.5	1.009 (9.5)	0.047 (42.7)	100/58	278/32	31	8	30	18	187/70	2.1	134/33	344/53	70/61	277/26
H	17/17	32.2	1.036 (11.1)	0.048 (18.2)	2/77	125/7	5	2	12	5	222/80	0.35	14/76	132/7	356/77	121/9
I	35/35	13.0	1.045 (2.7)	-0.388 (23.9)	347/71	117/13	6	3	8	4	218/80	5.7	357/74	117/8	3/72	119/8
J	23/23	25.2	1.014 (1.4)	-0.404 (34.6)	276/76	66/12	12	7	40	7	220/70	2	242/65	117/15	302/78	44/3
K	20/20	75.1	1.013 (8.5)	0.433 (35.5)	15/01	104/30	28	11	20	11	236/80	0.45	358/10	97/35	214/25	113/22
L	13/15	23.6	1.02 (6.1)	0.469 (32.3)	253/70	106/17	32	8	13	8	46/80	1.6	—	—	241/66	105/18
M	27/30	38.3	1.053 (16.6)	0.462 (18.9)	170/82	289/4	7	2	4	2	192/80	8.7	177/80	280/4	—	—
N	20/20	24.8	1.025 (9)	0.168 (27.3)	0/77	115/6	12	3	12	3	222/80	4	325/82	111/7	12/71	118/5
O	25/25	41.3	1.037 (1.9)	0.903 (22.7)	221/60	127/3	48	5	7	5	32/75	3.8	23/38	116/4	226/48	135/0
P	12/12	20.6	1.015 (46.7)	0.373 (23.9)	45/27	157/36	49	15	24	13	227/65	2.4	13/41	168/46	246/4	155/16
Q	9/14	23.3	1.012 (5.9)	0.032 (42.6)	339/83	109/4	16	6	19	6	226/71	3.8	215/49	117/5	344/81	122/7
R	22/26	23.8	1.022 (6.8)	0.113 (36.8)	8/84	125/2	10	3	13	3	28/86	6.6	23/71	119/2	302/89	115/1
S	24/24	22.1	1.019 (5.9)	0.011 (42.9)	306/74	108/14	8	5	11	5	182/75	2.5	338/68	99/12	302/75	113/15
T	21/30	6.8	1.01 (12)	-0.089 (44.3)	339/71	138/19	15	6	21	8	188/85	1.5	335/37	71/8	17/67	133/11
U	25/27	62.4	1.029 (10)	0.533 (17.4)	359/87	91/0	10	3	8	3	6/90	17	345/84	89/2	18/36	284/5
V	16/16	18.6	1.035 (16.6)	0.546 (28.5)	261/73	110/15	20	6	11	6	208/75	5.3	239/67	117/13	292/71	94/18
X	25/25	31.4	1.038 (9.5)	0.688 (21.0)	318/82	98/6	12	3	5	3	22/90	2.5	333/76	96/8	259/85	100/5
ρ	25/25	76.0	1.014 (9.5)	0.426 (34.3)	122/73	307/17	45	23	31	20	223/74	4.5	344/9	305/42	359/9	133/18
κ	8/12	33.1	1.066 (27.9)	0.352 (38.5)	301/62	136/28	5	4	7	3	211/66	1.2	297/67	120/23	295/58	121/31
δ	19/22	47.2	1.04 (10.2)	-0.639 (29.2)	70/71	307/11	7	5	24	5	250/88	2.4	72/69	285/18	66/71	331/2
ϵ	16/16	22.6	1.02 (6.2)	0.294 (32.6)	12/57	117/10	16	5	6	5	210/65	>14	—	—	12/57	117/10
λ	22	48.5	1.023 (7.2)	-0.682 (28.1)	138/67	240/5	8	5	35	5	192/35	4	141/58	43/5	129/75	269/12
μ	18/18	41.2	1.069 (25.2)	-0.195 (32.5)	48/75	314/1	8	5	14	6	80/89	3	15/77	124/4	62/68	319/5
ν	21	19.9	1.025 (6.6)	0.87 (26.6)	144/10	54/1	45	10	11	6	222/85	1	147/11	57/3	336/81	230/2
π	23	86.0	1.031 (6.4)	-0.428 (26.3)	116/14	210/15	8	6	8	6	220/71	0.6	123/18	218/15	115/10	207/13
θ	30/32	43.1	1.035 (8.3)	0.22 (22.0)	342/82	119/6	6	2	8	3	218/85	6.6	345/79	102/5	332/84	126/5
α	9/18	57.4	1.012 (16.1)	-0.018 (32.9)	176/63	318/22	39	16	43	20	33/82	4	29/01	298/11	144/55	14/24
σ	32	73.3	1.018 (6)	-0.592 (32.0)	123/17	32/2	8	7	21	8	226/65	0.8	122/10	213/2	129/22	37/3
τ	14/20	44.8	1.035 (12.7)	-0.475 (25.7)	184/75	286/3	4	4	12	3	33/81	5.5	169/77	274/3	195/71	296/4
ω	31	62.7	1.053 (20)	-0.671 (13.1)	108/0	18/49	6	4	20	3	27/90	3	107/2	16/45	292/2	33/32
ξ	24	71.6	1.025 (6.7)	-0.617 (28.0)	117/13	23/16	14	6	14	10	206/65	1.5	114/15	18/22	119/12	28/3

N , number of samples for mean parameters.

Bold type indicates inverse magnetic fabric sites.

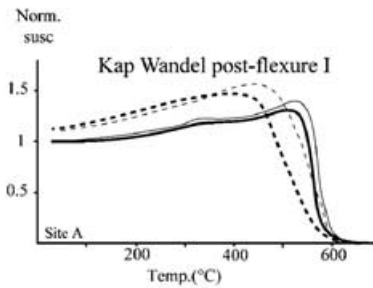
D/I, declination and inclination of AMS axes (geographical coordinates).

n , number of samples for flow estimates.

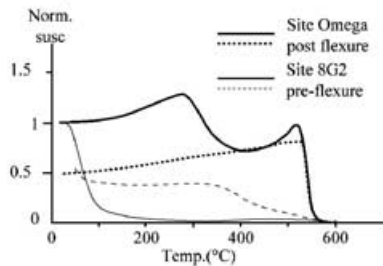
E1 and E2 are the 95 per cent confidence angles of AMS axes.

Dyke trend: azimuth, dip to the right direction, dip.

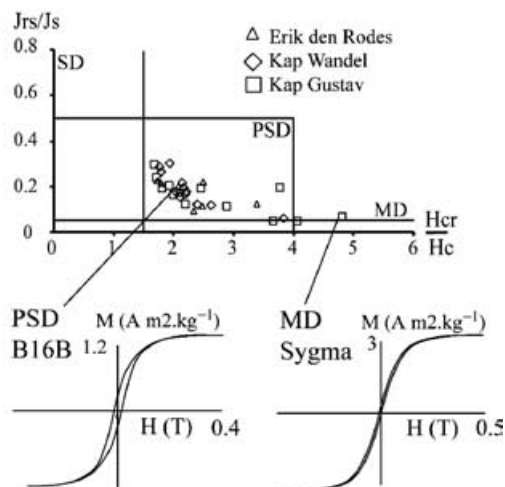
(a) K-T curves, Normal Fabric sites



(b) K-T curve, Inverse Fabric sites



(c) Hysteresis results



(d) Isothermal remanent magnetisation

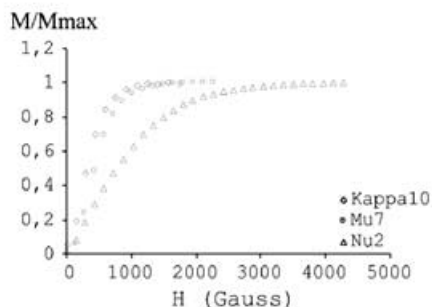


Figure 7. Example of rock magnetic results. (a) K - T curve under low field for normal fabric dykes: bold line under air; thin line under argon; dashed line indicates cooling. (b) K - T curves for two examples of inverse fabric, dashed line for cooling. (c) Day-type plot (Day *et al.* 1977) for the three zones, with typical hysteresis loops for pseudo-single-domain and multidomain grains. (d) Example of isothermal remanent magnetization curves. See details in text.

since we are focusing on the normal magnetic fabrics which are flow related.

Saturation of isothermal remanent magnetization (Fig. 7d) is typical of low-coercivity ferromagnetic minerals, except for the dyke ν , which contains a slight proportion of haematite. High-field hysteresis loops measured at the Saint-Maur Laboratory (IPGP, Paris) confirm the occurrence of low-coercivity ferromagnetic (*sensu lato*) grains. Typical pseudo-single-domain (PSD) loops were measured together with some quasi-multidomain (MD) loops (Fig. 7c). Hysteresis parameters are not dependent on dyke generation, the geographical position or the type of magnetic fabric. The entire data set defines a classic trend from PSD grains to MD grains, most probably due to a mixture of real PSD and MD grains with similar Ti substitution.

4.3 Magnetic susceptibility and ellipsoid

Site mean bulk magnetic susceptibility ranges from 6.8×10^{-3} to 86×10^{-3} SI, with a mean value of $(42 \pm 21) \times 10^{-3}$ SI (Table 2). Such values are indicative of rocks whose magnetic susceptibility is of mixed paramagnetic and ferrimagnetic origin, the ferrimagnetic contribution being the greatest (Rochette *et al.* 1992). Using the formula of Rochette *et al.* (1992), the contribution of paramagnetic silicates (the matrix) should not exceed 5×10^{-3} SI. Thus the ferrimagnetic particles are the main contributors to the magnetic susceptibility, with the exception of dyke T (Table 2).

Fig. 8 reports, for each studied transect, the mean magnetic parameters P' (degree of AMS) and T (shape factor) (Jelinek 1981). The Kap Wandel dykes display a low degree of AMS ($P' < 1.05$) and cluster in the oblate ellipsoidal field ($0 < T < 1$). Except for dyke I, the first- and second-generation dykes exhibit an oblate AMS ellipsoid. The third-generation dykes show moderately neutral ellipsoids with a very low degree of AMS ($P' < 1.04$). At Kap Gustav, the normal fabric dykes have a neutral ellipsoid on average, with anisotropies ranging from 1.01 to 1.07, whereas the inverse fabric dykes display a rather prolate magnetic fabric ($T < -0.3$) of low anisotropy ($P' < 1.05$, except for dyke ν).

4.4 Representative magnetic fabrics (Fig. 9)

The dyke σ exhibits a typical inverse magnetic fabric (*sensu* Rochette *et al.* 1999), with a good clustering of both K_1 and K_3 , which precludes any further possibility of determining the flow direction (eight dykes): the magnetic lineation corresponds to the dyke pole, while the magnetic foliation poles are horizontal within the dyke plane.

Site I displays a normal fabric, and yields well-clustered magnetic axes with no imbrication (the mean axes from each margin are not statistically different). Nevertheless, an important feature of such dykes is that the magnetic foliation plane is oblique on the dyke plane. This fabric could be interpreted by a normal-type fabric sheared during dyke emplacement (Rochette *et al.* 1991), bearing no information concerning the flow direction.

We obtain normal magnetic fabrics for 33 dykes (i.e. 75 per cent). Among them, two dykes show poorly grouped normal fabrics. No imbrication of the magnetic axes can be recognized in such sites (e.g. dyke JV15, which only bears a flow lineation). An imbrication of both magnetic axes is observed in four dykes, thus providing the most reliable magnetic configuration for flow determination (dyke JV16). In such cases, flow directions inferred from K_1 and K_3 can be compared and the result considered with good confidence.

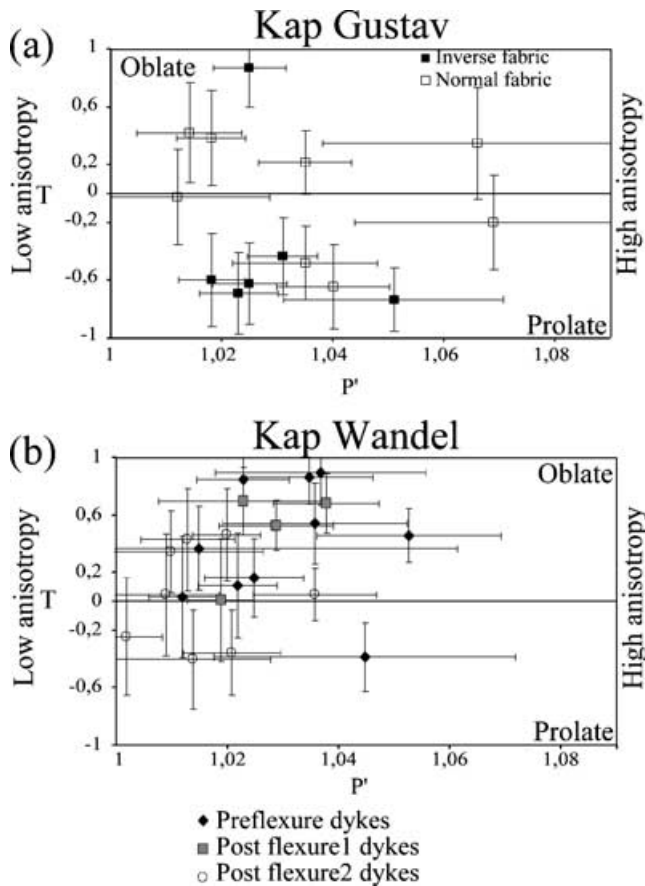


Figure 8. P' versus T plots for (a) the Kap Wandel and (b) the Kap Gustav sampling zones. Errors are quoted at 1σ .

Nevertheless, most of the measured dykes (25 out of 44, or 60 per cent) show only an imbrication of rather well-clustered magnetic foliation planes that are vertical and close to the dyke plane (dyke θ). Magnetic lineations are generally poorly constrained and scattered within the dyke plane, but with a mean orientation systematically close to the vertical, parallel to the zone axis of the magnetic foliation planes (Henry 1997). Finally, in four cases (dykes B, D, V, δ), we measured magnetic fabrics that were identical to the previously described ones (i.e. with an imbrication of the magnetic foliation planes at least; compare dykes V and dyke θ), but with a mean dyke plane that does not bisect the mean foliation planes.

4.5 Microtextural analysis

In a previous study (Callot *et al.* 2001a), 20 thin sections were cut within the magnetic plane of samples from normal fabric sites and 40 representative images were taken to analyse the rock texture, following a protocol using the Intercept software (Launeau & Robin 1996). To supplement this preliminary data set, 70 new photographs were processed from 32 new thin sections cut within the K_1 – K_2 and K_2 – K_3 planes from 17 cores. The results have been presented and discussed in detail in a previous paper (Geoffroy *et al.* 2002), and thus we only point out here the main results. We observed a variable agreement between plagioclase shape-preferred orientation—assumed to measure the flow-related texture at dyke margins (see discussion in Varga *et al.* 1998)—and the magnetic lineation.

The results show that the plagioclase phenocrysts are predominantly arranged within the magnetic foliation plane (K_1 – K_2), which

can thus be truly considered as providing an estimate of the flow plane orientation. For the Erik den Rødes dykes, we observe a good agreement within this plane between the plagioclase lineation and the K_1 , with less than 30° of angular deviation in ~ 60 per cent of cases (see Fig. 11a). It appears here that magnetic lineation is generally a good indicator of flow. On the contrary, for the Kap Wandel dykes, the deviation between K_1 and the plagioclase shape-preferred orientation within the magnetic foliation plane is greater than 45° in 60 per cent of the analysed cases, suggesting that either K_1 or K_2 may be considered as flow indicators.

5 FLOW DIRECTIONS INFERRED FROM MAGNETIC FABRICS

5.1 Flow vectors at the dyke scale

In this study flow directions are only inferred from sites with normal magnetic fabrics. In Fig. 9(b), we present several representative examples of flow-vector determinations taken from the three studied zones. As far as possible, we have tried to obtain a local flow vector for each measured sample (and for the pooled samples, a mean vector for each margin), and a mean flow vector for each margin. Wherever possible, both of these flow vectors were derived from the imbrication of the magnetic foliation plane (see Table 3).

The southernmost studied zone has already been investigated using the imbrication of magnetic lineation (Callot *et al.* 2001a), so here we can compare the flow directions obtained from both methodologies (i.e. lineation versus foliation methods). In the case of JV16 (Fig. 9b), both the local and mean flow vectors agree closely with a horizontal westward-directed flow, similar to the flow direction inferred from the magnetic lineation. Dyke JV15 presents poorly constrained AMS data that do not show any imbrication, and only a horizontal flow lineation was inferred (Callot *et al.* 2001a). Nevertheless, the southern margin yields a rather well-constrained flow direction derived from the imbrication of magnetic foliation, both at the plug scale and the margin scale, all consistent with the horizontal magnetic lineation of the dyke.

Almost 66 per cent of the dykes from the Kap Wandel area yield consistent flow estimates (see Table 3 and Fig. 9B). The flow vectors estimated from the pooled plugs are in general consistent with the mean flow vectors estimated from the mean magnetic axes of each margin. The flow directions are mostly horizontal and southwest directed, except for dyke L, which shows a northeastward flow, and dykes C and G which show downward- and upward-directed flow, respectively (Table 3). A remarkable feature of our results is the apparent contradiction between the horizontal flow vector, i.e. inferred from the magnetic foliation, and the on average vertical magnetic lineation.

The normal magnetic fabrics of the Kap Gustav dykes are apparently similar to those measured at Kap Wandel, with a generally well-defined imbrication of the magnetic foliation plane, and a better clustered vertical magnetic lineation (Fig. 9, dyke θ). However, in contrast to the Kap Wandel dykes, the flow vector estimates from Kap Gustav are of poorer quality, with large uncertainties, although the magnetic foliation imbrication is generally consistent with horizontal southwestward-directed flow. The few dykes that show reliable flow estimates yield horizontal and southward-directed flow directions.

Several dykes yield results that are in contradiction from one dyke margin to the other (dyke δ , B, D, H and V). These dykes present a well-defined imbrication of magnetic foliation planes, but the flow

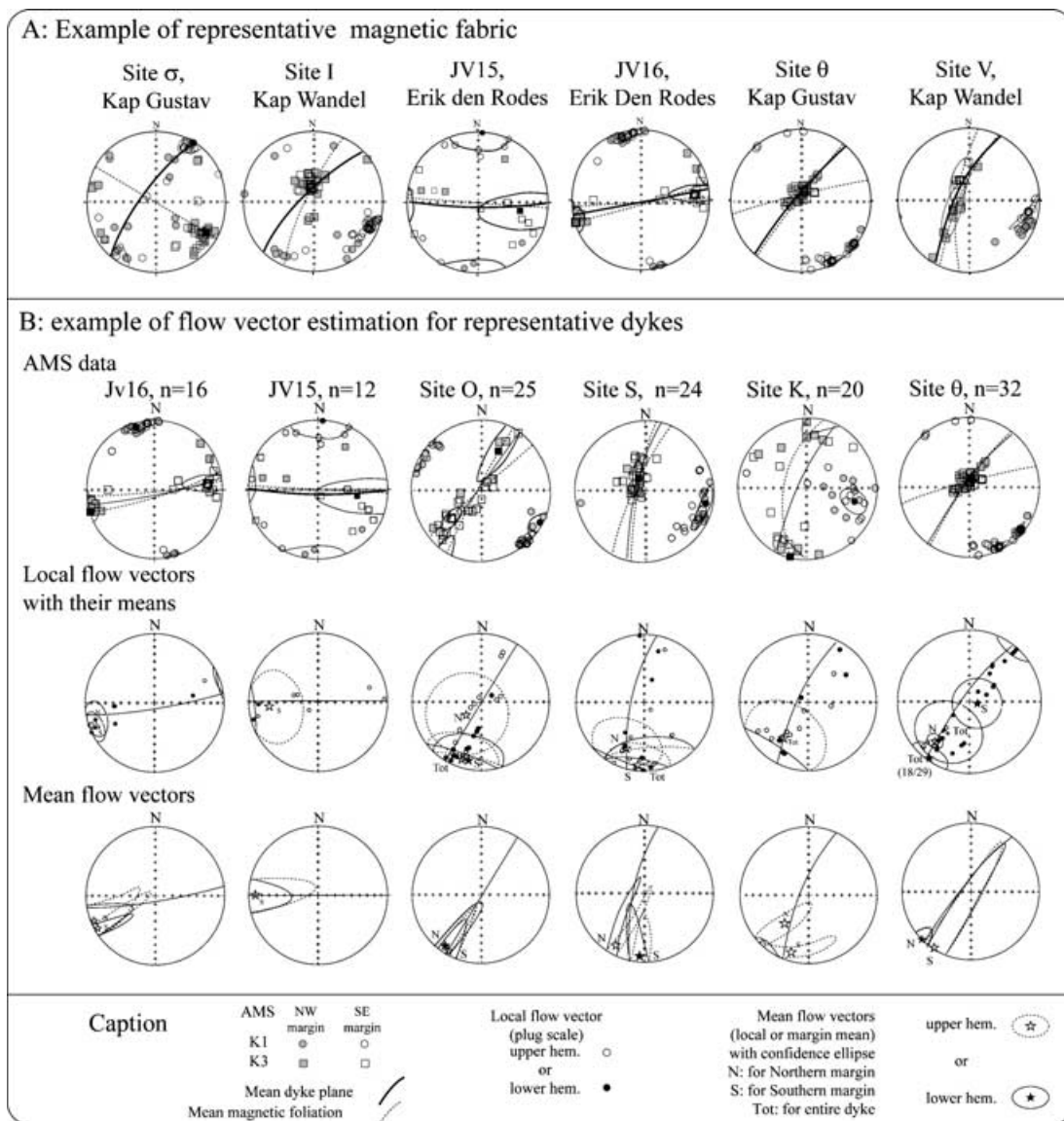


Figure 9. (a) Typical AMS configurations encountered; explanation in text. (b) Example of flow vector estimations. Upper row, AMS data; middle row, local (plug-scale) flow vectors with their means for each margin and for the entire dyke; lower row, flow vectors at the margin scale (compare with Fig. 6). Lower hemisphere projection.

vectors estimated at one margin are opposite to those obtained at the other margin, because the measured dyke plane does not bisect the two magnetic foliation planes from each margin. We thus are unable to estimate a consistent flow direction in this case, but the AMS data are apparently flow-related, with an imbrication of foliation consistent with a subhorizontal flow lineation.

5.2 General pattern of flow

The mean magnetic axes K_1 and K_3 of each normal-fabric site (see Table 2), are plotted in the dyke reference frame, i.e. the dyke is rotated to the vertical and along a north–south strike (Fig. 10) Rochette *et al.* (1991). In so doing, we obtain a spectacular clustering of the K_3 axes, which defines an imbrication of the magnetic foliation planes with respect to the dyke plane. The mean magnetic foliation poles for the entire data set are horizontal, being offset from the mean dyke pole by 6° anticlockwise and 10° clockwise

for the western and eastern margins respectively. This imbrication shows almost perfectly the expected mirror geometry (compare with Fig. 5(a); see Tauxe *et al.* 1998). This also illustrates the scattering of the magnetic lineations around the vertical mean, which delineates the average foliation plane. As described above, the magnetic lineations do not define any imbrication and present vertical means for each margin. Thus, the entire data set presents a magnetic texture which is remarkably consistent with a general horizontal and southward-directed flow direction, in agreement with the more scattered local and mean flow vectors.

6 DISCUSSION AND CONCLUSION

AMS measurements in dykes are used to determine the magma flow geometry and thus to draw conclusions about the emplacement mechanism and more generally on the geodynamic evolution of the studied system. These studies rely on the assumption that (1) the

Table 3. Flow vector estimates for the Kap Wandel and Kap Gustav dykes. Fv N(S) is the flow vector for the northern (southern) margin. Means of the local flow vectors are calculated on the northern (southern) margin, with 95 per cent confidence angle. Margin mean flow vectors are determined from the mean of the low-susceptibility axis (K_3) and the mean trend of each margin. Entries in *italic* are for reliable estimates of lineation and entries in **bold** are for reliable estimates of direction.

Dyke	Local flow vectors				Mean flow vectors			
	Fv N	α_{95}	Fv S	α_{95}	Total	α_{95}	Fv N	Fv S
A	32/5	15	167/–61	15	137/–61	37	237/37	215/–55
S	229/–30	37	202/6	41	214/–10	29	233/–8	211/5
U	222/–2	26	106/23	~90	220/5	12(17/24)	219/0	214/0
B	<i>288/–37</i>	49	<i>60/65</i>	66	<i>281/11</i>	<i>~90</i>	<i>258/2</i>	<i>78/0</i>
D	<i>28/20</i>	35	<i>221/–5</i>	54	<i>8/37</i>	73	<i>17/–60</i>	<i>187/77</i>
I	265/25	36	62/37	51	302/65	48	251/7	65/24
M	—	—	—	—	255/62	7	251/47	—
N	—	—	190/–44	70	212/–53	37	251/6	225/–25
O	256/–66	50	219/14	35	226/–13	35	249/3	240/0
P	110/–75	<i>~90</i>	87/44	<i>~90</i>	92/–1	<i>~90</i>	96/–53	258/14
Q	—	—	—	—	284/34	44	256/16	—
R	322/–72	34	104/32	~90	246/–22	41(12/21)	247/–36	230/18
V	<i>55/–65</i>	67	<i>57/22</i>	57	<i>56/–17</i>	52	<i>247/32</i>	<i>6/66</i>
X	238/14	21	200/–2	80	226/9	35(16/25)	228/–11	205/–44
C	343/74	68	49/52	16	37/63	25	49/70	57/51
F	244/–80	50	226/4	70	230/–48	48	233/–31	235/5
G	—	—	—	—	183/–66	48	—	157/–76
H	<i>253/–17</i>	82	<i>55/82</i>	<i>~90</i>	<i>256/27</i>	<i>~90</i>	<i>66/–11</i>	<i>68/15</i>
J	—	—	—	—	253/6	62	249/–2	—
K	244/–35	21	108/33	~90	241/–34	46	240/–42	240/–16
L	—	—	—	—	71/18	20	—	61/28
T	204/–7	66	216/9	11	213/5	20	215/–7	206/10
ρ	—	—	—	—	—	—	288/72	225/12
κ	6/23	28	227/37	18	279/56	49	223/25	226/32
δ	<i>251/24</i>	12	<i>78/–33</i>	19	<i>125/–48</i>	13	<i>250/22</i>	<i>70/–23</i>
ϵ	—	—	99/–60	13	—	—	—	87/–61
μ	255/–4	8	88/–20	12	—	—	76/4	259/8
θ	221/–27	12	209/36	12	207/46	37	227/–2	211/0
α	220/–2	35	—	—	—	—	219/13	—
τ	224/20	20	197/–31	65	238/–39	78	212/11	190/–65

petrofabric is coaxial to the flow fabric and (2) the magnetic fabric is a measure of the petrofabric. The first assumption is difficult to establish and is generally not discussed. The second corresponds in fact to the assumption that the magnetic lineation is a reliable estimate of the oxide preferred elongation, i.e. a measure of the flow lineation, and can be tested. Although a general agreement between external flow indicators and magnetic lineation is found in several studies, a number of studies show large discrepancies between those oriented lineations (Ellwood 1978; Baer 1995; Dragoni *et al.* 1997; Geoffroy *et al.* 2002). In normal magnetic fabric dykes with a planar magnetic texture the macroscopic magnetic lineation may express a composite texture (for instance a zone axis of planar texture for the Greenland dykes) rather than a true estimate of the grain shape orientation (Callot & Guichet 2003). As most dykes bear oblate magnetic fabrics, the geometric use of the magnetic foliation plane avoids any uncertainty about the significance of K_1 , and offers an interesting alternative. It nevertheless remains that each AMS measurement is a complex averaging of several sources of contrasted intensity and several types of anisotropy. The inherent complexity of a potentially turbulent magmatic system such as a dyke, together with the complexity of the measurement itself, precludes any automatic treatment of such data.

The flow directions are remarkably consistent and homogeneous along the 125 km of margin studied. Although the number of studied dykes is no more than 10 per cent of the total outcropping dykes,

we may confidently assume that the flow pattern can be broadly applied to the entire dyke swarm because we sampled dykes from each recognized generation. The first interesting result is that the flows are predominantly horizontal (Figs 10 and 11). The second point is that the flows are practically all directed southwestwards, i.e. away from the magma centres of Imilik. This flow pattern is persistent through time, since it concerns the three generations of intrusions with ages spanning over 4 Myr (Lenoir *et al.* 2002). This global flow pattern is remarkably consistent with the proposed model of a margin fed by lateral injection of dykes from a localized magma reservoir (Geoffroy 2001). Our data suggest that the entire flood basalt sequence could have been fed through the lateral injection of dykes from crustal magma chambers, followed by fissure eruptions at the topographic surface. This result stresses the enormous volume of magma that was transferred from deep-seated and localized melting zones in the mantle to the crust, through a very restricted number of magma reservoirs along the continental margin. Our result can be compared with the already published flow directions from the Isle of Skye (Inner Hebrides, Scotland, Geoffroy & Aubourg 1997; Herrero-Bervera *et al.* 2001), which belongs to an extinct Tertiary rift zone associated with the North Atlantic Volcanic Province (Speight *et al.* 1982; Hitchen & Ritchie 1993). Here, the lavas were fed by the horizontal flow of magma in dykes injected laterally from magma storage zones located beneath a central igneous complex.

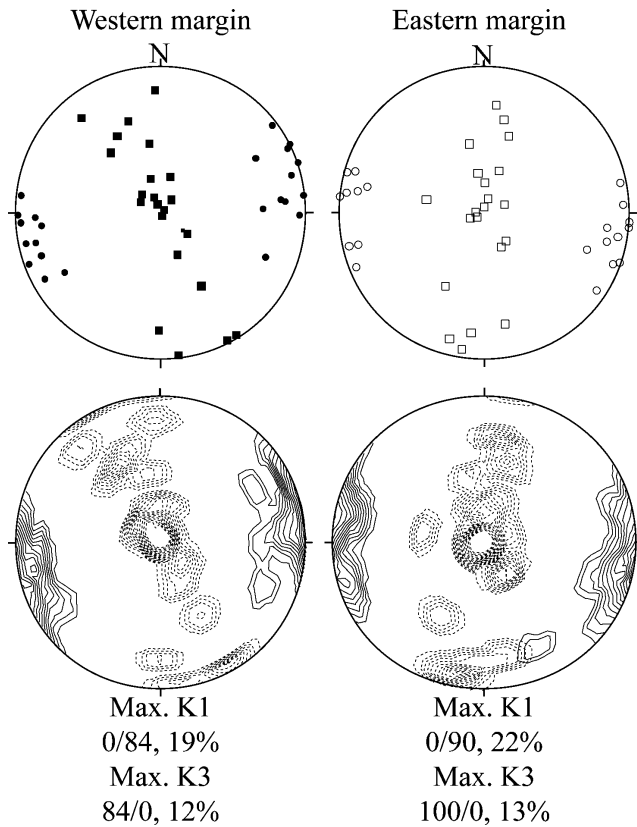


Figure 10. Plot of the mean AMS axes for each dyke margin, in dyke coordinates. Circles and continuous line, K_3 ; squares and dashed line, K_1 . Density contours incremented from 1 per cent. Note the spectacular imbrication of the mean magnetic foliation pole, which indicates a southward-directed flow for the entire data set (21 dykes shown).

To a large extent, these results compare well with the proposed model of Bhattacharji *et al.* (1996) for the feeding of the Deccan flood basalts. The Deccan lava pile was fed through the lateral flow of magmas within dyke swarms located in rift zones bordering the cratonic lithosphere (Narmada lineament). The systematic occurrence of a huge magma centre and associated dyke swarm in LIPs suggests a similar mode of feeding (see, for example, the Namibian margin, Bauer *et al.* 2000). Finally, the present results are remarkably similar to the model proposed for the magmatic growth of slow-spreading ridges (Lin *et al.* 1990), as observed in the sheeted complex of the Troodos ophiolite (Staudigel *et al.* 1992; Abelson *et al.* 2001). We should bear in mind that the Greenland flow pattern is established at a relatively shallow palaeodepth of about 2–4 km (Hansen 1995), which is also comparable to the dyke swarms emplaced at mid-oceanic ridges. In all these examples, large igneous provinces and slow-spreading ridges, the focused ascent of the hot mantle material and melting seems to govern the whole magmatic accretion of the crust.

ACKNOWLEDGMENTS

The crew of the polar ship *Vagabond* (E. Brossier, F. Pinczon du Sel) is greatly thanked for their professionalism and kindness. The field party was composed of F. Delbart, J. P. Gélard (1999); F. Delbart, X. Lenoir and R. Aite (2000); and F. Delbart, G. Féraud, H. Bertrand and Y. Gunnel (2001). The authors gratefully acknowledge M. LeGoff for the use of the magnetic apparatus of the Saint-Maur-IPGP Laboratory, and N. Catel (ENS Laboratory) for geochemical analyses. This paper benefited from thorough reviews by B. Henry and an anonymous reviewer. Dr M. S. N. Carpenter, a professional translator, is acknowledged for post-editing the manuscript. This work was supported by the GDR ‘Marges’ and benefited from the

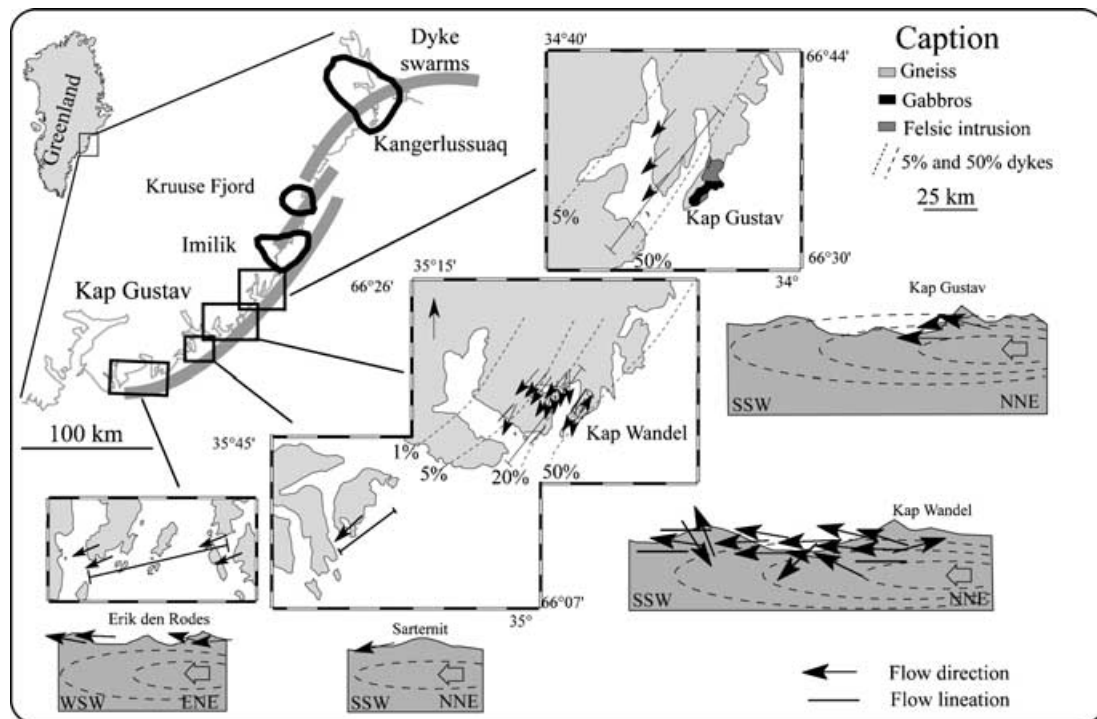


Figure 11. Synthesis of flow directions obtained for the East Greenland volcanic margin, on map and on vertical cross-sections along-strike.

logistic support of the French Polar Institute (IFRTP programme 290).

REFERENCES

- Abelson, M., Baer, G. & Agnon, A., 2001. Evidence from gabbro of the Troodos ophiolite for lateral magma transport along a slow-spreading mid-ocean ridge, *Nature*, **409**, 72–75.
- Anderson, D.L., 1994. The sublithospheric mantle as the source of continental flood basalts; the case against the continental lithosphere and plume head reservoir, *Earth planet. Sci. Lett.*, **123**, 269–280.
- Arbaret, L., Diot, H., Bouchez, J.L., Lespinasse, P. & De Saint-Blanquat P., 1997. Analogue 3D simple shear experiments of magmatic biotite sub-fabric, in *Granite: from Segregation of Melt to Emplacement Fabrics*, pp. 129–143, eds Bouchez, J.L., Hutton, D.H.W. & Stephens, W.E., Kluwer Academic Publishers, Dordrecht.
- Aubourg, C., Giordano, G., Mattei, M. & Speransa, S., 2002. Magma flow in sub-aqueous rhyolitic dikes inferred from magnetic fabric analysis (Ponza Island, W. Italy), *Phys. Chem. Earth*, **27**, 1223–1272.
- Baer, G., 1995. Fracture propagation and magma flow in segmented dykes: Field evidences and fabric analyses, in *Physics and Chemistry of Dykes*, pp. 125–143, eds Baer, G. & Heimann, A., Balkema, Rotterdam.
- Bauer, K. *et al.*, 2000. Deep structure of the Namibia continental margin as derived from integrated geophysical studies, *J. geophys. Res.*, **105**, 28 829–28 853.
- Bhathal, R.S., 1971. Magnetic anisotropy in rocks, *Earth Sci. Rev.*, **7**, 227–253.
- Bhattacharji, S., Chatterjee, N., Wampler, J.M., Nayak, P.N. & Deshmukh, S.S., 1996. Indian intraplate and continental margin rifting, lithospheric extension, and mantle upwelling in Deccan flood basalt volcanism near the K/T boundary: evidence from mafic dikes swarms, *J. Geol.*, **104**, 379–388.
- Blanchard, J.-P., Boyer, P. & Gagny, C., 1979. Un nouveau critère de mise en place dans une caisse filonienne: le ‘pincement’ des minéraux aux épontes, *Tectonophysics*, **53**, 1–25.
- Borradaile, G.J. & Henry, B., 1997. Tectonic application of magnetic susceptibility and its anisotropy, *Earth Sci. Rev.*, **42**, 49–93.
- Bouchez, J.-L., 1997. Granite is never anisotropic: an introduction to AMS studies of granitic rocks, in *Granite: from Segregation of Melt to Emplacement Fabrics*, pp. 95–112, eds Bouchez, J.L., Hutton, D.H.W. & Stephens, W.E., Kluwer Academic Publishers, Dordrecht.
- Callot, J.P., 2002. Origine, structure et développement des marges volcaniques: l'exemple du Groënland. Interaction manteau-lithosphère en contexte de panache, *PhD Thesis*, Université Pierre et Marie Curie, Paris VI.
- Callot, J.P. & Guichet, X., 2003. Rock texture and magnetic lineation in dykes: a simple analytical model, *Tectonophysics*, **366**, 207–222.
- Callot, J.P., Geoffroy, L., Aubourg, C., Pozzi, J.P. & Mege, D., 2001a. Magma flow direction of shallow dykes from the East Greenland margin inferred from magnetic fabric studies, *Tectonophysics*, **335**, 313–329.
- Callot, J.P., Grigné, C., Geoffroy, L. & Brun, J.-P., 2001b. Development of volcanic passive margin: 2D laboratory models, *Tectonics*, **20**, 148–159.
- Callot, J.P., Geoffroy, L. & Brun, J.P., 2003. Development of volcanic passive margin: 3D laboratory models, *Tectonics*, **21**, 1052, doi:10.1029/2001TC901019.
- Canon-Tapia, E., Walker, G.P.L. & Herrero-Bervera, E., 1997. The internal structure of lava flows—insights from AMS measurements II: Hawaiian pahoehoe, toothpaste lava and a'a, *J. Volc. Geotherm. Res.*, **76**, 19–46.
- Clift, P.D., Carter, A. & Hurford, A.J., 1998. The erosional and uplift history of the NE Atlantic passive margins: constraints on a passive plume, *J. geol. Soc. Lond.*, **155**, 787–800.
- Coffin, M.F. & Eldholm, O., 1994. Large igneous provinces: crustal structure, dimensions, and external consequences, *Rev. Geophys.*, **32**, 1–36.
- Courtillot, V., Jaupart, C., Manighetti, I., Tapponnier, P. & Besse, J., 1999. On causal links between flood basalts and continental break-up, *Earth planet. Sci. Lett.*, **166**, 177–195.
- Day, R., Fuller, M.D. & Schmidt, V.A., 1977. Hysteresis properties of titanomagnetites: grain size and composition dependence, *Phys. Earth planet. Int.*, **13**, 260–266.
- Dragoni, M., Lanza, R. & Tallarico, A., 1997. Magnetic anisotropy produced by magma flow: theoretical and experimental data from Ferrar dolerite sills (Antarctica), *Geophys. J. Int.*, **128**, 230–240.
- Eldholm, O. & Grue, K., 1994. North Atlantic volcanic margins: dimensions and production rates, *J. geophys. Res.*, **99**, 2955–2968.
- Eldholm, O., Skogseid, J., Planke, S. & Gladzenko, P., 1995. Volcanic margin concept, in *Rifted Ocean–Continent Boundaries*, pp. 1–16, ed. Banda, E., Kluwer Academic Publishers, Dordrecht.
- Ellwood, B.B., 1978. Flow and emplacement direction determined for selected basaltic bodies using magnetic susceptibility anisotropy measurements, *Earth planet. Sci. Lett.*, **41**, 254–264.
- Fitton, J.G., Saunders, A.D., Larsen, L.M., Hardarson, B.S. & Norry, M.J., 1998. Volcanic rocks from the Southeast Greenland margin at 63°N: composition, petrogenesis, and mantle source, in *Proc. Ocean Drilling Program, Scientific Results*, pp. 503–533, eds Saunders, A.D., Larsen, H.C. & Wise, S.W.J., Ocean Drilling Program, College Station, TX.
- Fleitout, L., Froidevaux, C. & Yuen D., 1986. Active lithosphere thinning, *Tectonophysics*, **132**, 271–278.
- Fram, M.S. & Leshner, C.E., 1997. Generation and polybaric differentiation of East Greenland early Tertiary flood basalts, *J. Petrol.*, **38**, 261–275.
- Geoffroy, L., 1998. Diapirisme et extension intra-plaque: cause ou conséquence?, *C. R. Acad. Sci., Paris*, **326**, 267–273.
- Geoffroy, L., 2001. The structure of volcanic margins: some problematics from the North Atlantic/Baffin Bay system, *Mar. Petrol. Geol.*, **18**, 463–469.
- Geoffroy, L. & Aubourg, C., 1997. Magma injection around plume-related high-level ultramafic bodies in Skye Island: a study with AMS, in EUGIX [abstract].
- Geoffroy, L., Callot, J.P., Aubourg, C. & Moreira, M., 2002. Divergence between magnetic and plagioclases linear fabrics in dykes: a new approach for defining the flow vector using magnetic foliation, *TerraNova*, **14**, 183–190.
- Graham, J.W., 1954. Magnetic susceptibility anisotropy, an unexploited petrofabric element, *Geol. Soc. Am. Abstr. Program*, **65**, 1257–1258.
- Hansen, K., 1995. Thermotectonic evolution of a rifted continental margin: fission track evidence from the Kangerdlussuaq area, SE Greenland, *TerraNova*, **8**, 458–469.
- Hargraves, R.B., Johnson, D. & Chan, C.Y., 1991. Distribution anisotropy: the cause of AMS in igneous rocks?, *Geophys. Res. Lett.*, **18**, 2193–2196.
- Henry, B., 1997. The magnetic zone axis: a new element of magnetic fabric for the interpretation of magnetic lineation, *Tectonophysics*, **271**, 325–331.
- Herrero-Bervera, E., Walker, G.P.L., Canon-Tapia, E. & Garcia, M.O., 2001. Magnetic fabric and inferred flow direction of dikes, conesheets and sill swarms, Isle of Skye, Scotland, *J. Volc. Geotherm. Res.*, **106**, 195–201.
- Hext, G., 1963. The estimation of second-order tensor, with related tests and designs, *Biometrika*, **50**, 353–357.
- Hill, R.I., 1991. Starting plumes and continental break-up, *Earth planet. Sci. Lett.*, **104**, 398–416.
- Hillhouse, J.W. & Wells, R.E., 1991. Magnetic fabric, flow direction, and source area of the lower Miocene Peach Spring Tuff in Arizona, California and Nevada, *J. geophys. Res.*, **96**, 12 443–12 460.
- Hinz, K., 1981. Hypothesis on terrestrial catastrophes: wedges of very thick oceanward dipping layers beneath passive margins—their origin and palaeoenvironment significance, *Geol. Jahrbuch*, **22**, 345–363.
- Hitchen, K. & Ritchie, J.D., 1993. New K–Ar ages, and a provisional chronology, for the offshore part of the British Tertiary Igneous Province, *Scot. J. Geol.*, **29**, 73–85.
- Holmes, A., 1918. The basaltic rocks of the Arctic region, *Mineral. Mag.*, **18**, 180–223.
- Housen, B.A.C. & Van der Pluijm, B., 1993. Composite magnetic anisotropy fabric: experiments, numerical models and implication for the quantification of rock fabrics, *Tectonophysics*, **220**, 1–12.
- Jelinek, V., 1978. Statistical processing of anisotropy of magnetic susceptibility measured on groups of specimens, *Stud. Geophys. Geod.*, **22**, 50–62.
- Jelinek, V., 1981. Characterisation of the magnetic fabric of rocks, *Tectonophysics*, **79**, T63–T67.

- Ježek, J., Schulmann, K. & Segeth, K., 1996. Fabric evolution of rigid inclusions in mixed coaxial and simple shear flow, *Tectonophysics*, **257**, 203–221.
- Karson, J.A. & Brooks, C.K., 1999. Structural and magmatic segmentation of the Tertiary east Greenland volcanic rifted margin, in *Continental Tectonics*, Geological Society of London Special Publication 164, pp. 313–318, eds Ryan, P. & McNicoll, C., Geological Society, London.
- Kerr, A.C., 1994. Lithospheric thinning during the evolution of large igneous provinces: a case study from the North Atlantic Tertiary province, *Geology*, **22**, 1027–1030.
- Khan, M.A., 1962. Anisotropy of magnetic susceptibility in some igneous and metamorphic rocks, *J. geophys. Res.*, **67**, 2873–2885.
- Klausen, M.B., 1999. Structure of rift-related igneous systems and associated crustal structures, PhD Thesis, University of Copenhagen.
- Klausen, M.B. & Larsen, H.C., 2002. East Greenland dyke swarm and its role in continental break-up, in *Volcanic Rifted Margins*, Geological Society of America Special Publication 362, pp. 133–158, eds Menzies, M.A., Klemperer, S., Ebinger, C.J. & Baker, J., Geological Society of America, Washington, DC.
- Knight, M.D. & Walker, G.P.L., 1988. Magma flow direction in dykes of the Koolau complex, Oahu, determined from magnetic fabric studies, *J. geophys. Res.*, **93**, 4301–4319.
- Korenaga, J., Holbrook, W.S., Kent, D.V., Kelemen, P.B., Detrick, R.S., Larsen H.C., Hopper, J.R. & Dahl-Jensen, T., 2000. Crustal structure of the southeast Greenland margin from joint refraction and reflection seismic tomography, *J. geophys. Res.*, **105**, 21 591–21 614.
- Larsen, H.C., 1978. Offshore continuation of East Greenland dyke swarm and North Atlantic Ocean formation, *Nature*, **274**, 220–223.
- Launeau, P. & Robin, P.-Y.F., 1996. Fabric analyses using the intercept method, *Tectonophysics*, **267**, 91–119.
- Lenoir, X., Féraud, G. & Geoffroy, L., 2002. *Short-time Flexure of the East Greenland Rifted Margin from Direct $^{40}\text{Ar}/^{39}\text{Ar}$ Dating of Basaltic Dykes*, EGS, Nice.
- Lienert, B.R., 1991. Monte Carlo simulation of errors in the anisotropy of magnetic susceptibility: a second-rank symmetric tensor, *J. geophys. Res.*, **96**, 19 539–19 544.
- Lin, J., Purdy, G.M., Schouten, H., Sempere, J.C. & Zervas, C., 1990. Evidence from gravity data for focused accretion along the Mid-Atlantic ridge, *Nature*, **334**, 627–632.
- Moreira, M., Geoffroy, L. & Pozzi, J.-P., 1999. Ecoulement magmatique dans les dykes du point chaud des Açores: étude préliminaire par anisotropie de susceptibilité magnétique ASM dans l'île de San Jorge, *C. R. Acad. Sci., Paris*, **329**, 15–22.
- Morgan, W.J., 1972. Plate motion and deep mantle convection, *Geol. Soc. Am. Bull.*, **132**, 7–22.
- Myers, J.S., 1980. Structure of the coastal dyke swarm and associated plutonic intrusions of East Greenland, *Earth planet. Sci. Lett.*, **46**, 407–418.
- Nicolas, A., 1992. Kinematics in magmatic rocks with special reference to gabbro, *J. Petrol.*, **33**, 891–915.
- Nielsen, T.F.D., 1978. The Tertiary dyke swarm of the Kangerdlussuaq area, East Greenland, *Cont. Mineral. Petrol.*, **67**, 63–78.
- Nielsen, T.K., Larsen, H.C. & Hopper, J.R., 2002. Contrasting rifted margin styles south of Greenland: implication for mantle plume dynamics, *Earth planet. Sci. Lett.*, **200**, 271–286.
- Palmer, H.C. & MacDonald, W.D., 1999. Anisotropy of magnetic susceptibility in relation to source vents of ignimbrites: empirical observations, *Tectonophysics*, **307**, 207–218.
- Richards, M.A., Duncan, R.A. & Courtillot, V., 1989. Flood basalts and hot-spot tracks: plume head and tails, *Science*, **246**, 103–107.
- Rochette, P., Jenatton, L., Dupuy, C., Boudier, F. & Reuber, I., 1991. Emplacement modes of basaltic dykes in the Oman ophiolite: evidence from magnetic anisotropy with reference to geochemical studies, in *Ophiolite Genesis and the Evolution of the Oceanic Lithosphere*, pp. 55–82, eds Peters, T.J., Nicolas, A. & Coleman, R.J., Kluwer, Dordrecht.
- Rochette, P., Jackson, M. & Aubourg, C., 1992. Rock magnetism and the interpretation of anisotropy of magnetic susceptibility, *Rev. Geophys.*, **30**, 209–226.
- Rochette, P., Aubourg, C. & Perrin, M., 1999. Is this magnetic fabric normal? A review and case studies in volcanic formations, *Tectonophysics*, **307**, 219–234.
- Scarrow, J.H. & Cox, K.G., 1995. Basalts generated by decompressive adiabatic melting of mantle plume: a case study from the Isle of Skye, NW Scotland, *J. Petrol.*, **36**, 3–22.
- Sinton, C.W. & Duncan, R.A., 1998. ^{40}Ar - ^{39}Ar ages of the lavas from the southeast Greenland margin, ODP leg 152, and the Rockall plateau, DSDP leg 81, in *Proc. Ocean Drilling Program, Scientific Results*, pp. 479–501, eds Saunders, A.D., Larsen, H.C. & Wise, S.W.J., Ocean Drilling Program, College Station, TX.
- Speight, J.M., Skelhorn, R.R., Sloan, T. & Knapp, R.J., 1982. The dyke swarm of Scotland, in *Igneous Rocks of the British Isles*, pp. 449–459, ed. Sutherland, D.S., John Wiley, New York.
- Stacey, F.D., 1960. Magnetic anisotropy of igneous rocks, *J. geophys. Res.*, **65**, 2429–2442.
- Staudigel, H.G., Gee, J.S., Tauxe, L. & Varga, R.J., 1992. Shallow intrusive direction of sheeted dikes in the Troodos ophiolite: anisotropy of magnetic susceptibility and structural data, *Geology*, **20**, 841–845.
- Stephenson, A., Sadikun, S. & Potter, D.K., 1986. A theoretical and experimental comparison of the anisotropies of magnetic susceptibility and remanence in rocks and minerals, *Geophys. J. R. astr. Soc.*, **84**, 185–200.
- Tarling, D.H. & Hrouda, F., 1993. *The Magnetic Anisotropy of Rocks*, Chapman and Hall, London.
- Tauxe, L., Gee, J.S. & Staudigel, H., 1998. Flow direction in dikes from anisotropy of magnetic susceptibility data: the bootstrap way, *J. geophys. Res.*, **103**, 17 775–17 790.
- Tegner, C., Duncan, R.A., Bernstein, S., Brooks, C.K., Bird, D.K. & Storey M., 1998. ^{40}Ar - ^{39}Ar geochronology of Tertiary mafic intrusions along the East Greenland rifted margin: relation to flood basalts and the Iceland hotspot track, *Earth planet. Sci. Lett.*, **156**, 75–88.
- Torsvik, T.H.J., Mosar, J. & Eide, E.A., 2001. Cretaceous–Tertiary geodynamics: a North Atlantic exercise, *Geophys. J. Int.*, **146**, 850–866.
- Varga, R.J., Gee, J.S., Staudigel, H. & Tauxe, L., 1998. Dykes surfaces lineations as magma flow indicators within the sheeted dyke complex of the Troodos ophiolite, Cyprus, *J. geophys. Res.*, **103**, 5241–5256.
- Wager, L.R. & Deer, W.A., 1938. A dyke swarm and crustal flexure in East Greenland, *Geol. Mag.*, **75**, 39–46.
- White, R.S. & McKenzie, D.P., 1989. Magmatism at rift zones: the generation of volcanic continental margins and flood basalts, *J. geophys. Res.*, **94**, 7685–7729.
- White, R.S. & McKenzie, D.P., 1995. Mantle plume and flood basalts, *J. geophys. Res.*, **100**, 17 543–17 585.